



# The transiently ordered regions in intrinsically disordered ExsE are correlated with structural elements involved in chaperone binding

Zhida Zheng<sup>a</sup>, Dejian Ma<sup>b</sup>, Timothy L. Yahr<sup>c</sup>, Lingling Chen<sup>a,\*</sup>

<sup>a</sup> Department of Molecular and Cellular Biochemistry, Indiana University, Bloomington, IN 47405, USA

<sup>b</sup> Department of Chemistry, Indiana University, Bloomington, IN 47405, USA

<sup>c</sup> Department of Microbiology, University of Iowa, Iowa City, IA 52242, USA

## ARTICLE INFO

### Article history:

Received 11 November 2011

Available online 25 November 2011

### Keywords:

Dynamics of ExsE

The ExsE–ExsC interaction

NMR studies

Intrinsically disordered proteins

T3SS substrate

## ABSTRACT

Many Gram-negative bacteria utilize a type III secretion system (T3SS) to deliver protein effectors to target host cells. Transcriptional control of T3SS gene expression is generally coupled to secretion through the release of a regulatory protein. T3SS gene expression in *Pseudomonas aeruginosa* is regulated by extracellular secretion of ExsE. ExsE is a small 81 residue protein that appears to lack a stable structural core as indicated by previous studies. In this study, we employed various NMR methods to characterize the structure of ExsE alone and when bound to its secretion chaperone ExsC. We found that ExsE is largely unfolded throughout the polypeptide chain, belonging to a class of proteins that are intrinsically disordered. The unfolded, extended conformation of ExsE may expedite efficient secretion through the narrow path of the T3SS secretion channel to activate gene expression in a timely manner. We also found that the structurally flexible ExsE samples through conformations with localized structurally ordered regions. Importantly, these transiently ordered elements are related to the secondary structures involved in binding ExsC based on a prior crystal structure of the ExsC–ExsE complex. These findings support the notion that preexisting structured elements facilitate binding of intrinsically disordered proteins to their targets.

© 2011 Elsevier Inc. All rights reserved.

## 1. Introduction

Many Gram-negative bacteria use a type III secretion system (T3SS) to establish effective infection [1–4]. *Pseudomonas aeruginosa* is an important human pathogen that causes pneumonia and urinary tract infections in hospitalized individuals, and uses the T3SS mechanism to translocate toxins into host cells [5]. Genes associated with the T3SS include those encoding the secretion machinery, the regulatory components, the effectors, and effector-specific chaperones. Transcriptional regulation of T3SS gene expression is linked to secretion of a T3SS substrate ExsE [6,7]. Specifically, the T3SS genes of *P. aeruginosa* are under direct control of the transcription factor ExsA [8]. The DNA binding activity of ExsA is controlled by a partner-switching mechanism involving ExsC, ExsD and ExsE [6,7,9–11]. Under non-inducing conditions for T3SS gene expression (high  $\text{Ca}^{2+}$  concentration or the absence of host cells), ExsA forms a complex with the anti-activator ExsD, and ExsE interacts with the secretion chaperone ExsC. Under these conditions the higher binding affinity of ExsC for ExsE (dissociation constant  $K_d$  of 1 nM) relative to ExsD ( $K_d$  of 18 nM) confines ExsC to the thermodynamically

more stable ExsC–ExsE complex [12]. In response to calcium-limitation or contact with host cells, ExsE is secreted. The resulting decrease in intracellular ExsE favors formation of the ExsD–ExsC complex and dissociation of the ExsD–ExsA complex. The released ExsA then binds to the promoters to upregulate the T3SS gene expression.

The secretion-mediated expression of T3SS genes in *P. aeruginosa* is initiated upon secretion of ExsE. To facilitate secretion through the long path of the narrow T3SS channel (20–30 Å in diameter [13,14]), most secreted proteins are maintained in a non-native, unfolded conformation by their secretion chaperones [15]. Intracellular ExsE is recognized by and forms a complex with its secretion chaperone ExsC. In most cases where structural information exists, the chaperone-binding domains (CBDs) of secreted substrates including SptP (*Salmonella*), YopE (*Yersinia*), and YopN (*Yersinia*) are wrapped around their respective chaperones in an extended, unfolded conformation [16–18]. Similarly, in the stable ExsE–ExsC interface, ExsE is in the fully extended conformation, and two signature  $\beta$  strands at both the N- and C-termini of the ExsE polypeptide pair with two symmetry-related five-stranded  $\beta$  sheets of dimeric ExsC [19].

In contrast to the characterized nonglobular conformation in the chaperone bound state, limited structural information is available on the chaperone-binding domains of the secreted proteins in the absence of the secretion chaperone. Most likely, the CBDs lack a

\* Corresponding author. Address: Department of Molecular and Cellular Biochemistry, 212 S. Hawthorne Dr. Simon Hall 400A, Indiana University, Bloomington, IN 47405, USA. Fax: +1 812 855 6082.

E-mail address: [linchen@indiana.edu](mailto:linchen@indiana.edu) (L. Chen).

stable core structure and their conformations are highly dynamic, reminiscent of proteins that are intrinsically disordered [20–22]. Intrinsically disordered proteins (IDP) exist as dynamic ensembles of various conformations. IDP's are biologically important with known roles including regulation, recognition, and signaling and control pathways. A previous analysis suggests that ExsE contains little secondary or tertiary structures and is structurally flexible [12]. In this study, we further characterized the solution conformation of ExsE using a variety of NMR techniques. We identified regions that are partially ordered in the largely unstructured ExsE polypeptide. Furthermore, we found that these regions are correlated with those that adopt secondary structures when ExsE binds to ExsC. These findings suggest the importance of pre-existing ordered structured in binding of intrinsically disordered proteins to their targets.

## 2. Materials and methods

### 2.1. Protein purification

The gene encoding ExsE was PCR-amplified and cloned into pTWIN1 (New England Biolabs) via *NdeI* and *EcoRI* restriction sites, to generate a fusion protein of ExsE and the chitin-binding protein. The final ExsE protein contains seven additional amino acids (EFLEGSS, 768 Da) at the carboxyl terminus. *Escherichia coli* BL21(DE3) was transformed with pTWIN1 for protein expression. To express  $^{15}\text{N}$ -labeled ExsE, cells were grown in M9 medium at 37 °C until OD<sub>600</sub> reached 0.4, and expression of ExsE was induced with 0.4 mM isopropyl 1-thio- $\beta$ -D-galactopyranoside (IPTG) for 9 h. To purify ExsE, cells were lysed in buffer A (20 mM TrisCl, pH 7.0, 500 mM NaCl, and 1 mM EDTA), and the cleared lysate was loaded onto a chitin column (New England Biolabs). The column was washed extensively with buffer A, and then incubated with buffer B (buffer A plus 40 mM dithiothreitol (DTT), pH 8.5) overnight at 4 °C to remove the chitin-binding protein. The eluted ExsE was concentrated, and dialyzed to buffer C (50 mM imidazole, pH 7.0, 200 mM NaCl, 0.5 mM EDTA, and 1 mM  $\beta$ -mercaptoethanol) for further purification using a gel filtration column (Superdex 75, Amersham Biosciences). The purified ExsE (~95% by SDS-PAGE) was concentrated to ~0.3 mM, and dialyzed to buffer D (50 mM Na-phosphate, pH 6.85, 150 mM NaCl) for NMR study.

### 2.2. NMR spectroscopy

NMR experiments were conducted at 298 K on VNMRS 600 MHz and 800 MHz NMR spectrometers (Agilent Technologies). Both were equipped with HCN cold probes with an actively shielded z-axis gradient. Pulse sequences from the BioPack pulse sequence library within VnmrJ software were used for all the NMR experiments. 2D  $^1\text{H}$ – $^{15}\text{N}$  heteronuclear correlation spectrum (HSQC) was collected using (800, 128) complex data points in the ( $^1\text{H}$ ,  $^{15}\text{N}$ ) dimensions with spectral width of 12.0 ( $^1\text{H}$ ) and 36.0 ppm ( $^{15}\text{N}$ ) and carrier frequencies on  $\text{H}_2\text{O}$  proton signal, and 120 ppm, in the  $^1\text{H}$  and  $^{15}\text{N}$  dimensions, respectively [23]. Relaxation delay of 1 s and 8 scans per free induction decay (FID) were used. 3D  $^{15}\text{N}$  edited NOESYHSQC was collected using (874, 100, 32) complex data points in the  $^1\text{H}$ , indirect  $^1\text{H}$  and  $^{15}\text{N}$  dimensions, respectively. Spectral widths of 12.0, and 30.9 ppm were used for  $^1\text{H}$  and  $^{15}\text{N}$  dimensions. Relaxation delay of 1 s and 8 scans per FID were used with NOE mixing time of 150 ms. 3D  $^{15}\text{N}$ -edited TOCSYHSQC was recorded with (616, 80, 60) complex data points in the  $^1\text{H}$  indirect  $^1\text{H}$  and  $^{15}\text{N}$  dimensions, respectively. Spectral widths of 12.0, and 30.0 ppm were used for  $^1\text{H}$  and  $^{15}\text{N}$  dimensions. Relaxation delay of 1 s and 4 scans per FID were used with 50 ms spin lock (mix) time.

### 2.3. Backbone dynamics measurements

$^{15}\text{N}$   $T_1$ ,  $T_2$ , and  $\{^1\text{H}\}$ – $^{15}\text{N}$  heteronuclear NOE were acquired with 512 and 64 complex data points in the  $^1\text{H}$  and  $^{15}\text{N}$  dimensions, respectively [24]. The carrier frequencies and spectral widths were the same as HSQC. The longitudinal relaxation time,  $T_1$ , were recorded using 8 delay values, 0.02, 0.1, 0.2, 0.4, 0.6, 0.9, 1.3, and 1.9 s with 3 s relaxation delay and 8 scans per FID. The transverse relaxation time,  $T_2$ , were measured with 8 delay values, 0.03, 0.07, 0.11, 0.15, 0.19, 0.25, 0.33, and 0.49 s with 2.5 s relaxation delay and 8 scans per FID.  $\{^1\text{H}\}$ – $^{15}\text{N}$  heteronuclear NOE was collected with 16 scans with and without a 3 s  $^1\text{H}$  saturation period in an interleaved fashion.

All NMR experiments were acquired on the 600 MHz spectrometer, except the 2D HSQC and 3D NOESY HSQC of the ExsE alone sample, which were collected using the 800 MHz spectrometer. NMR data was processed using NMRPipe and NMRDraw [25] and analyzed using NMRPipe and Sparky 3 [26].

## 3. Results

### 3.1. ExsE is intrinsically disordered

ExsE is 81 amino acids in length, lacks of stable secondary structures, and resembles random coil conformations in solution based on circular dichroism (Fig. S1A). Whereas ExsE is rapidly degraded to small undetectable peptides by SDS-PAGE following a brief treatment with subtilisin, stable fragments were obtained for ExsC using the same treatment (Fig. S1B). The limited stability of ExsE towards proteolytic digestion suggests that it either lacks of stable tertiary fold or adopts a highly dynamic structure. The  $^1\text{H}$ – $^{15}\text{N}$  HSQC NMR spectra showed that the amide proton chemical shifts of ExsE collapse in a narrow range of 7.8–8.6 ppm (Fig. 1A), consistent with the absence of secondary structures in ExsE. Together, these biochemical and biophysical observations suggest that the solution structure of ExsE is highly dynamic with limited secondary structural components.

The narrow span in the  $^1\text{H}$  dimension of the HSQC spectra may suggest nonspecific aggregation of ExsE, because backbone amine groups of polypeptides in nonspecific aggregates most likely have the similar chemical environments and their chemical shifts are not resolved. However, the  $^{15}\text{N}$  resonances of ExsE are dispersed and the resultant  $^1\text{H}$ – $^{15}\text{N}$  HSQC cross peaks are well resolved (Fig. 1A). For the ExsE construct used in this study, 83  $^1\text{H}$ – $^{15}\text{N}$  cross peaks would be expected as a result of seven extra residues at the C-terminus of the expressed ExsE and five Pro residues that do not contain an amino proton. From the  $^1\text{H}$ – $^{15}\text{N}$  HSQC spectra, a total of 78 distinguishable cross peaks can be identified, indicating that most of backbone amine groups in ExsE are in unique chemical environments and that ExsE does not form a nonspecific aggregate. Based on analyses of 3D  $^{15}\text{N}$ -edited TOCSY and NOESY data, 68 resonances have been assigned with amino acid sequences, including 67 residues (the C-terminal S88 causing two resonances S88 and S88') (Fig. 1A).

ExsE is highly dynamic throughout the polypeptide chain, as indicated by backbone dynamic analysis on relaxation times  $T_1$  and  $T_2$  of  $^{15}\text{N}$  and the  $\{^1\text{H}\}$ – $^{15}\text{N}$  heteronuclear NOEs. The reorientation of individual N–H bond vectors with the overall tumbling rate of the protein molecule is associated with the  $\{^1\text{H}\}$ – $^{15}\text{N}$  heteronuclear NOEs; a negative NOE reflects the rapid reorientation of the backbone N–H bond vector. Strikingly, most of the resonances in the  $\{^1\text{H}\}$ – $^{15}\text{N}$  heteronuclear spectra are negative as shown in Fig. S2A, indicating highly flexible backbone conformations throughout the ExsE polypeptide. The  $\{^1\text{H}\}$ – $^{15}\text{N}$  NOE signals with their corresponding amino acid sequences are summarized in Fig. 2A. The global dynamic nature of ExsE is also supported by

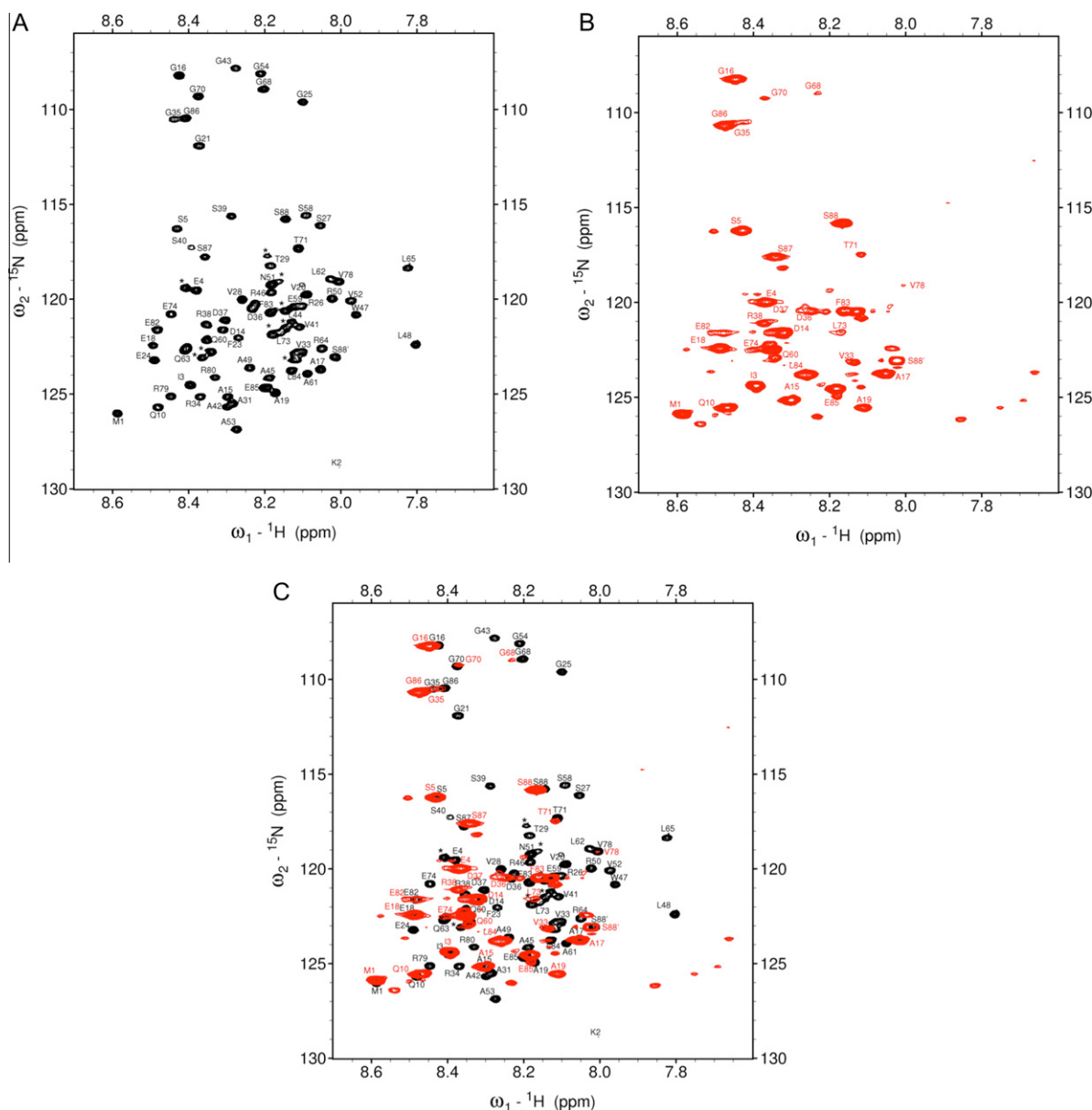


**Fig. 1.** (A)  $^1\text{H}$ - $^{15}\text{N}$  HSQC spectrum of ExsE alone (in black). (B)  $^1\text{H}$ - $^{15}\text{N}$  HSQC spectrum of ExsE in the presence of ExsC (in red), 29 residues with resonances could be identified. (C) Overlap of the  $^1\text{H}$ - $^{15}\text{N}$  HSQC spectra from ExsE alone (A) and ExsE-ExsC complex (B). The resonance assignments are labeled with the one-letter-code of the amino acids and the sequential numbers. Peaks labeled with asterisk sign (\*) are not been assigned. (For interpretation of the references to color in this figure legend, the reader is referred to the web version of this article.)

analysis of relaxation rates of the backbone amide group shown in Fig. 2B–C. Increasing values in  $T_2$ , the transverse relaxation time, suggest a more flexible environment surrounding the resonant nuclei. The well-folded 76-residue ubiquitin, with a comparable molecular size of ExsE, has an average  $T_2$  value of 0.18 s (at the same magnetic field of 600 MHz used for ExsE) for residues involved in forming stable core structure [27]. In comparison,  $T_2$  values for most of the ExsE residues are much higher at  $\sim 0.25$  s (Fig. 2B), suggesting that ExsE does not contain a stable structural fold. Although dynamic by nature, however, ExsE samples through conformations containing localized structured elements. Positive NOEs, reflecting decreased reorientation of the N–H bond vectors in respect to the overall tumbling of ExsE, are found for residues V28, A42, L44, A45, W47, L48, N51, A61, L62, and L65 (Fig. 2A and Fig. S2A). These findings indicate that some local regions in the globally unstructured ExsE may possess residual or transient structure. It is noteworthy that most of the residues with positive

NOEs correspond to regions that form helical structures, helix  $\alpha 1$  of residue 41–51 and helix  $\alpha 2$  of residues 58–67, in the ExsC-bound ExsE [19]. Furthermore, NOEs from nonsequential residues, indicative of secondary and tertiary structure in the protein, were observed (Fig. 3). Notably, Fig. 3 shows the nonsequential, inter-residue NOE signals between W47 and residues of A45, N51, and V52, indicating transient ordering of these residues in a helix-like conformation. Taken together, while ExsE is largely extended and highly dynamic along the entire polypeptide chain, it samples through conformations with localized ordered regions.

### 3.2. Conformation of ExsE upon binding to ExsC

The binding of ExsE to ExsC is in the slow exchange regime on the NMR time scale, consistent with the stable ExsC–ExsE complex detected by ITC ( $K_d$  of 1 nM) [12]. The presence of ExsC caused large resonance-specific chemical shift perturbations in the

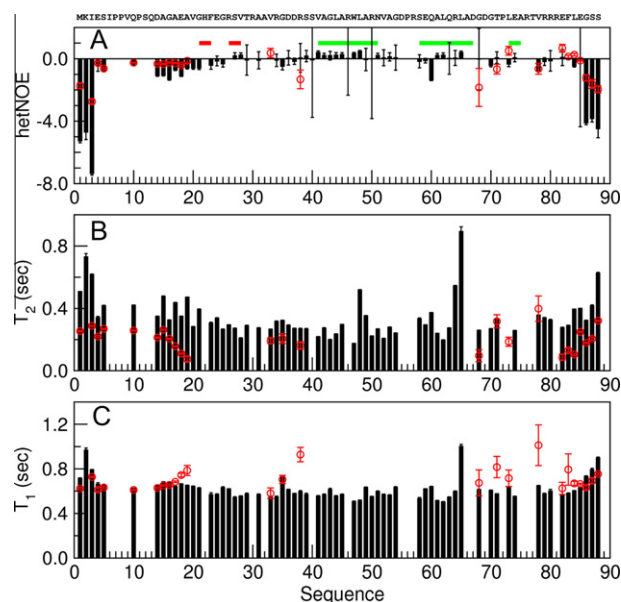


**Fig. 2.** Summary of backbone dynamic analysis. (A)  $\{^1\text{H}\}$ - $^{15}\text{N}$  heteronuclear NOEs; (B)  $^{15}\text{N}$  transverse relaxation time  $T_2$ ; (C)  $^{15}\text{N}$  longitudinal relaxation time  $T_1$ . The ExsE sequence is shown above (A). Results of ExsE alone are shown in black bars, and those of ExsE in the presence of ExsC are in red circles. The green and red horizontal bars in panel (A) respectively represent  $\alpha$  helix and  $\beta$  strand conformations in the crystal structure of ExsC-ExsE complex [19]. (For interpretation of the references to color in this figure legend, the reader is referred to the web version of this article.)

$^1\text{H}$ - $^{15}\text{N}$  HSQC NMR spectra of  $^{15}\text{N}$ -labeled ExsE, indicating a specific interaction between ExsC and ExsE. Changes in chemical shift on  $^1\text{H}$ - $^{15}\text{N}$  HSQC, as a result of complex formation, may be used to map residues in the macromolecular interface; however, it is not applicable in the ExsE-ExsC interaction. In the presence of ExsC, many ExsE resonances in  $^1\text{H}$ - $^{15}\text{N}$  HSQC were broadened and the intensities were reduced (Fig. 1B), most likely due to the slow tumbling rate of the large ExsE-ExsC complex (46.5 kDa). Only 30 resonances can be assigned with 29 amino acid residues (the C-terminal S88 giving rise to two resonances). Most assigned

resonances correspond to residues clustered at the N- and C-termini of ExsE (residues 1–20, and 70–88), and a region between residues 33 and 38.

For those resonance-assigned ExsE residues in the ExsC-ExsE complex, particularly those located at both termini of ExsE, their  $\{^1\text{H}\}$ - $^{15}\text{N}$  heteronuclear NOEs were negative (Fig. S2B and Fig. 2A), suggesting that both the N- and C-termini of ExsE remain structurally flexible in the ExsC-bound form.  $T_2$  for the well folded catabolite activator protein (CAP, 47 kDa), similar in size to the ExsC-ExsE complex, is  $\sim 0.03$  s (at the same magnetic field of 600 MHz used for ExsE) [28]. For residues at both ExsE termini, the  $T_2$  values are mostly around 0.2 s (Fig. 2B), and the high  $T_2$  values, consistent with negative NOEs, suggest flexible conformations for both ExsE termini. Presumably, structurally flexible regions in a stable complex like ExsC-ExsE ( $K_d$  of 1 nM [12]) are less likely at the intermolecular interface, so both ExsE termini do not contact ExsC. In sum, although our NMR studies on the ExsC-bound ExsE were not able to identify the ExsC binding site on ExsE, they show that both N- and C-termini of ExsE were not involved in interacting with ExsC. Importantly, the dynamic, unbound N-terminus of ExsE in the ExsC-bound form is functionally significant because it contains the T3SS secretion signal [29]. Thus, ExsC binding does not interfere with the subsequent recognition of ExsE by the T3SS machinery.

#### 4. Discussion

ExsE, a secreted substrate of the T3SS and a regulator of T3SS gene expression in *P. aeruginosa*, is structurally dynamic and intrinsically disordered. Previous analytical ultracentrifugation studies found that ExsE (9.4 kDa) exists as monomer. By gel filtration, however, the 88-residue ExsE corresponds to a spherical protein of 29 kDa [12]. In comparison, a polypeptide of 100 residues is estimated to behave hydrodynamically like a 29 kDa spherical protein when it adopts extended conformation with some content of secondary structure, and like a 40 kDa spherical protein when it is in coiled-like conformation with residual and highly flexible structure [22]. Thus, the large hydrodynamic volume suggests that the conformation of ExsE contains residual rather than persistent secondary structure, and resembles the coiled-like conformation. The lack of a stable structural core in the coiled-like conformation is in

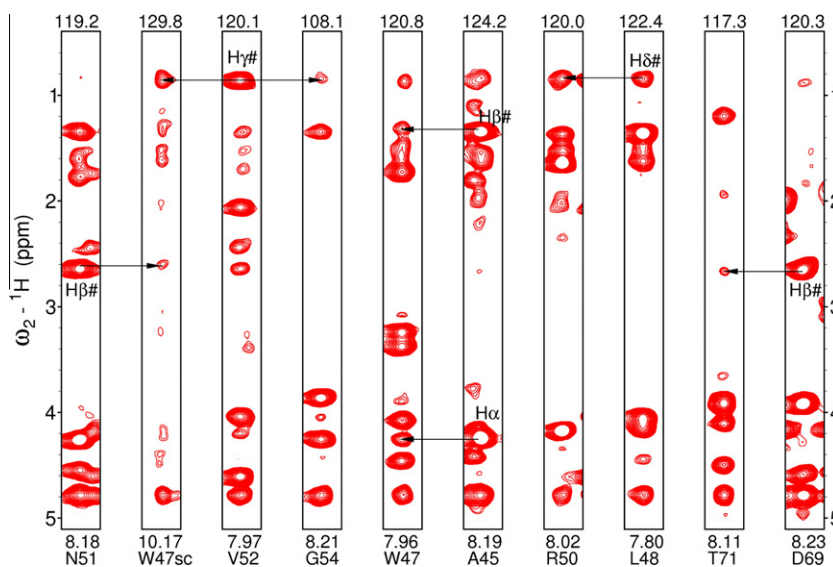


**Fig. 3.** Non-sequential NOE assignment of ExsE alone from the  $^{15}\text{N}$ -edited 3D NOESY data. The  $^{15}\text{N}$  and amide  $^1\text{H}$  chemical shifts of the residue are shown on the top and the bottom of the strip plot, respectively. The assigned residues are also labeled at the bottom. The indirect  $^1\text{H}$  dimension is shown as vertical axis. Among the signals shown, only those involved in the non-sequential NOE are labeled with the assignment. The intra- and sequential NOE signals are not labeled. The non-sequential NOE crosspeaks are indicated by the arrows.



line with the limited proteolysis study, which showed that ExsE was rapidly and completely degraded (Fig. S1B). The absence of signature features for the secondary structures in CD (Fig. S1A) indicates that no stable secondary structures persist in ExsE. Finally, the backbone dynamic analyses ( $T_1$ ,  $T_2$ , and heteronuclear NOE) indicate a highly flexible structure along the ExsE polypeptide with a few localized ordered elements. Together, these analyses indicate that ExsE is largely unfolded along the entire length of the polypeptide and is structurally flexible.

The existence of preformed structure in intrinsically disordered proteins appears to be important in their binding to target partners. In a study of surface antigen of Hepatitis B virus preS1, it was shown that the prestructured motifs in the largely disordered preS1 are correlated with the site of its binding to the hepatocyte receptor [30]. For the ribosomal protein S4, two regions in its largely unfolded N-terminus adopt transiently ordered structure: one such preordered structure aligns the side chains of two consecutive Arg residues in parallel towards the solvent, while the other forms a nascent poly-Pro turn [31]. These regions with preordered structure, highly conserved in sequence, are proposed to be the binding site for interacting with RNA or other ribosomal proteins. Lastly, a region in the largely unstructured 73-residue transactivation domain (TAD) of p53 is populated with an amphipathic helix [32], and is stabilized in a similar helical conformation when bound to target proteins [33,34]. The hydrophobic face of the amphipathic helix is proposed to be the recognition motif for the diverse regulators that interact with the p53 TAD. Our dynamic analysis on the backbone amides of ExsE shows that transient structural elements localized in residues 42–51 and 61–65 are located in the regions that form helix  $\alpha 1$  (residues 41–51) and  $\alpha 2$  (residues 58–67) when ExsE is bound to ExsC (refer to Fig. 2A) [19]. Notably, the conformation of residue W47 is stabilized as indicated by positive heteronuclear NOEs for both the backbone amide group (with a heteronuclear NOE value of 0.33) and side chain indole ring N $\pi$ H group (with a heteronuclear NOE value of 0.18, see Fig. S2A insert), and by the inter-residue NOEs from non-sequential residues (A45, N51, and V52). Furthermore, the pattern of the nonsequential NOEs is reminiscent of a helical conformation, suggesting that W47 is transiently involved in helix-like conformations. Intriguingly, in the crystal structure of the ExsC<sub>2</sub>–ExsE complex [19], W47 of ExsE is located in the middle of an 11-residue helix  $\alpha 1$  that interacts with a hydrophobic groove lined with ExsC residues from  $\alpha 2$  (F69, L72, F75, H78, W79 and F82) and from  $\alpha 3$  (H121, F124, W125, and L128). In particular, W47 of ExsE interacts with F75 and H78 of ExsC  $\alpha 2$ , and L48 of ExsE with F124, W125, and L128 of ExsC  $\alpha 3$ . Interestingly, the intermolecular hydrophobic interactions are rather dynamic, as the interfacing ExsE residues are structurally flexible and are not resolved in three of the six complexes in the asymmetric unit in the crystal. Positive NOEs are also associated with residues that form the two signature  $\beta$  strands ( $\beta 2$  of residues 25–31 and  $\beta 3$  of residues 75–81) that interact with ExsC. Each ExsE  $\beta$  strand adds to the five-stranded  $\beta$  sheet in the ExsC monomer, and despite their sequence difference, the two ExsE  $\beta$  strands interact with the two identical ExsC  $\beta$  sheets in the same manner [19]. Moreover, these interactions with ExsC via the  $\beta$  structures are stable as their conformations are conserved in all six complexes. In sum, the transiently ordered regions in the structurally dynamic ExsE are stabilized to form secondary structural elements when ExsE binds to ExsC, suggesting that the preformed structures are important in mediating binding of the largely unfolded ExsE to its target ExsC. In binding ExsC, ExsE is expected to lose the conformational entropy. Consistently, ITC studies show that  $\Delta S$  for the binding reaction is negative ( $-11$  J/mol) and the binding ( $K_d = 1$  nM) is driven by a large enthalpic release ( $-3.15 \times 10^4$  kJ/mol) (data not shown). In comparison, binding between the two well-folded ExsC and ExsD proteins ( $K_d = 15$ –

27 nM) is entropy favorable ( $\Delta S = 9.4$  J/mol) and with a smaller enthalpic release ( $-7.5 \times 10^3$  kJ/mol) (data not shown).

In addition to the chaperone binding region, most secreted proteins contain effector functions that subrogate the host defense system once in the host cytoplasm. The effector domain does not interact with the secretion chaperone but rather adopts a native conformation that is catalytically active in the chaperone bound state [17]. The well-formed effector domain needs to unfold prior to traversing through the long narrow T3SS channel ( $\sim 80$  Å in length and  $\sim 20$ – $30$  Å in diameter [13,14]), and the active unfolding has been shown to be driven by ATP hydrolysis [13]. Here we show that ExsE alone is largely unstructured throughout the entire polypeptide chain, is stable as a monomer, and does not form large aggregates. The lack of a globular structure may expedite efficient secretion of ExsE from bacterial cytoplasm in a timely manner to ensure rapid activation of T3SS genes.

## Appendix A. Supplementary data

Supplementary data associated with this article can be found, in the online version, at doi:10.1016/j.bbrc.2011.11.070.

## References

- [1] C.J. Hueck, Type III protein secretion systems in bacterial pathogens of animals and plants, *Microbiology and Molecular Biology Reviews* 62 (1998) 379–433.
- [2] J.E. Galan, A. Collmer, Type III secretion machines: bacterial devices for protein delivery into host cells, *Science* 284 (1999) 1322–1328.
- [3] G.V. Plano, J.B. Day, F. Ferracci, Type III export: new uses for an old pathway, *Molecular Microbiology* 40 (2001) 284–293.
- [4] P. Ghosh, Process of protein transport by the type III secretion system, *Microbiology and Molecular Biology Reviews* 68 (2004) 771–795.
- [5] J.T. Barbieri, J. Sun, *Pseudomonas aeruginosa* ExoS and ExoT, *Reviews of Physiology Biochemistry and Pharmacology* 152 (2004) 79–92.
- [6] M.L. Urbanowski, G.L. Lykken, T.L. Yahr, A secreted regulatory protein couples transcription to the secretory activity of the *Pseudomonas aeruginosa* type III secretion system, *Proceedings of the National Academy of Sciences of the United States of America* 102 (2005) 9930–9935.
- [7] A. Rietsch, I. Vallet-Gely, S.L. Dove, J.J. Mekalanos, ExsE, a secreted regulator of type III secretion genes in *Pseudomonas aeruginosa*, *Proceedings of the National Academy of Sciences of the United States of America* 102 (2005) 8006–8011.
- [8] D.W. Frank, The exoenzyme S regulon of *Pseudomonas aeruginosa*, *Molecular Microbiology* 26 (1997) 621–629.
- [9] M.L. McCaw, G.L. Lykken, P.K. Singh, T.L. Yahr, ExsD is a negative regulator of the *Pseudomonas aeruginosa* type III secretion regulon, *Molecular Microbiology* 46 (2002) 1123–1133.
- [10] N. Dasgupta, G.L. Lykken, M.C. Wolfgang, T.L. Yahr, A novel anti-anti-activator mechanism regulates expression of the *Pseudomonas aeruginosa* type III secretion system, *Molecular Microbiology* 53 (2004) 297–308.
- [11] E.D. Brutinel, C.A. Vakulskas, T.L. Yahr, ExsD inhibits expression of the *Pseudomonas aeruginosa* type III secretion system by disrupting ExsA self-association and DNA binding activity, *Journal of Bacteriology* 192 (2010) 1479–1486.
- [12] Z. Zheng, G. Chen, S. Joshi, E.D. Brutinel, T.L. Yahr, L. Chen, Biochemical characterization of a regulatory cascade controlling transcription of the *Pseudomonas aeruginosa* type III secretion system, *Journal of Biological Chemistry* 282 (2007) 6136–6142.
- [13] Y. Akeda, J.E. Galan, Chaperone release and unfolding of substrates in type III secretion, *Nature* 437 (2005) 911–915.
- [14] T.C. Marlovits, T. Kubori, A. Sukhan, D.R. Thomas, J.E. Galan, V.M. Unger, Structural insights into the assembly of the type III secretion needle complex, *Science* 306 (2004) 1040–1042.
- [15] C.E. Stebbins, J.E. Galan, Priming virulence factors for delivery into the host, *Nature Reviews Molecular Cell Biology* 4 (2003) 738–743.
- [16] C.E. Stebbins, J.E. Galan, Maintenance of an unfolded polypeptide by a cognate chaperone in bacterial type III secretion, *Nature* 414 (2001) 77–81.
- [17] S.C. Birtalan, R.M. Phillips, P. Ghosh, Three-dimensional secretion signals in chaperone-effector complexes of bacterial pathogens, *Molecular Cell* 9 (2002) 971–980.
- [18] F.D. Schubot, M.W. Jackson, K.J. Penrose, S. Cherry, J.E. Tropea, G.V. Plano, D.S. Waugh, Three-dimensional structure of a macromolecular assembly that regulates type III secretion in *Yersinia pestis*, *Journal of Molecular Biology* 346 (2005) 1147–1161.
- [19] N.J. Vogelaar, X. Jing, H.H. Robinson, F.D. Schubot, Analysis of the crystal structure of the ExsC ExsE complex reveals distinctive binding interactions of the *Pseudomonas aeruginosa* type III secretion chaperone ExsC with ExsE and ExsD, *Biochemistry* 49 (2010) 5870–5879.
- [20] V.N. Uversky, J.R. Gillespie, A.L. Fink, Why are “natively unfolded” proteins unstructured under physiologic conditions?, *Proteins* 41 (2000) 415–427.

- [21] A.K. Dunker, C.J. Brown, J.D. Lawson, L.M. Iakoucheva, Z. Obradovic, Intrinsic disorder and protein function, *Biochemistry* 41 (2002) 6573–6582.
- [22] V.N. Uversky, A.K. Dunker, Understanding protein non-folding, *Biochimica et Biophysica Acta* 1804 (2010) 1231–1264.
- [23] L.E. Kay, P. Keifer, T. Saarinen, Pure absorption gradient enhanced heteronuclear single quantum correlation spectroscopy with improved sensitivity, *Journal of the American Chemical Society* 114 (1992) 10663–10665.
- [24] N.A. Farrow, R. Muhandiram, A.U. Singer, S.M. Pascal, C.M. Kay, G. Gish, S.E. Shoelson, T. Pawson, J.D. Forman-Kay, L.E. Kay, Backbone dynamics of a free and phosphopeptide-complexed Src homology 2 domain studied by  $^{15}\text{N}$  NMR relaxation, *Biochemistry* 33 (1994) 5984–6003.
- [25] F. Delaglio, S. Grzesiek, G.W. Vuister, G. Zhu, J. Pfeifer, A. Bax, NMRPipe: a multidimensional spectral processing system based on UNIX pipes, *Journal of Biomolecular NMR* 6 (1995) 277–293.
- [26] T.D. Goddard, D.G. Kneller, SPARKY 3, University of California, San Francisco.
- [27] R. Bruschweiler, S.F. Lienin, T. Bremi, B. Brutscher, R.R. Ernst, Anisotropic intramolecular backbone dynamics of ubiquitin characterized by NMR relaxation and MD computer simulation, *Journal of the American Chemical Society* 120 (1998) 9870–9879.
- [28] S.R. Tzeng, C.G. Kalodimos, Dynamic activation of an allosteric regulatory protein, *Nature* 462 (2009) 368–372.
- [29] G.R. Cornelis, F. Van Gijsegem, Assembly and function of type III secretory systems, *Annual Review of Microbiology* 54 (2000) 735–774.
- [30] S.W. Chi, D.H. Kim, S.H. Lee, I. Chang, K.H. Han, Pre-structured motifs in the natively unstructured preS1 surface antigen of hepatitis B virus, *Protein Science* 16 (2007) 2108–2117.
- [31] E.W. Sayers, R.B. Gerstner, D.E. Draper, D.A. Torchia, Structural preordering in the N-terminal region of ribosomal protein S4 revealed by heteronuclear NMR spectroscopy, *Biochemistry* 39 (2000) 13602–13613.
- [32] H. Lee, K.H. Mok, R. Muhandiram, K.H. Park, J.E. Suk, D.H. Kim, J. Chang, Y.C. Sung, K.Y. Choi, K.H. Han, Local structural elements in the mostly unstructured transcriptional activation domain of human p53, *Journal of Biological Chemistry* 275 (2000) 29426–29432.
- [33] P.H. Kussie, S. Gorina, V. Marechal, B. Elenbaas, J. Moreau, A.J. Levine, N.P. Pavletich, Structure of the MDM2 oncoprotein bound to the p53 tumor suppressor transactivation domain, *Science* 274 (1996) 948–953.
- [34] M. Uesugi, G.L. Verdine, The alpha-helical FXXPhiPhi motif in p53: TAF interaction and discrimination by MDM2, *Proceedings of the National Academy of Sciences of the United States of America* 96 (1999) 14801–14806.